Wind Modeling and Lateral Control for Automatic Landing

W.E. Holley*
Dept. of Mechanical Engineering, Oregon State University, Corvallis, Oregon
and
A.E. Bryson Jr.†
Dept. of Aeronautics and Astronautics, Stanford University, Stanford, Calif.

For the purposes of aircraft control system design and analysis, the wind can be characterized by a mean component which varies with height and by turbulent components which are described by the von Karman correlation model. The aircraft aerodynamic forces and moments depend linearly on uniform and gradient gust components obtained by averaging over the aircraft's length and span. The correlations of the averaged components are then approximated by the outputs of linear shaping filters forced by white noise. The resulting model of the crosswind shear and turbulence effects is used in the design of a lateral control system for the automatic landing of a DC-8 aircraft.

Introduction

ONE of the more challenging problems facing an autopilot designer is the synthesis of feedback logic which will achieve the desired attitude and position of an aircraft at touchdown in the presence of turbulent crosswinds. During the approach phase of an automatic landing, the desired flight path is maintained by heading slightly into the prevailing crosswind ("crabbing"). However, at touchdown, the aircraft centerline must be aligned with the runway to prevent lateral skidding of the wheels on the landing gear. The transition from the approach attitude to the touchdown attitude, termed the "decrab maneuver," is usually carried out by the pilot, using the rudder to reduce the heading deviation, and ailerons to dip the windward wing tip sightly so as to maintain the lateral position in the presence of the resulting aerodynamic sideslip. When visibility is reduced to the point where the pilot cannot maintain the required visual reference, it is desirable to perform the decrab maneuver automatically.

In order to carry out an effective automatic landing, accurate information on the aircraft's attitude and position is required. In the last several years, accurate and reliable navigation systems have been developed to provide this information. Such systems include inertially augmented ILS systems,[1,2] microwave landing systems, MLS,[3] and various attitude reference systems.[4] It is anticipated that further improvements in system accuracy and reliability will be made in the future.

Touchdown errors in automatic landing are also caused by turbulent winds. In contrast with the navigation errors, there is little hope of reducing these disturbances. In fact, as landing speeds are lowered, as in STOL aircraft applications, the wind effects become more pronounced.

Briefly stated, the goal of this research is to develop systematic techniques for the design of feedback control logic which will minimize the effects of the wind disturbances. To achieve this goal, the problem is broken into three parts. First, a reasonably accurate description of the wind and corresponding turbulence is developed; the variation of the mean wind and the turbulence parameters with height is included in this model. Second, the aerodynamic effects of the mean wind and the turbulence on the aircraft are modeled. We endeavored to develop models which are as simple as possible, and yet retain the essential features of the wind shear and turbulence effects. Third, the resulting models of the wind and its aerodynamic effects are used in conjunction with optimal control design techniques to determine control logic which minimizes the expected values of the output errors.

Presented as Paper 75-1077 at the AIAA Guidance and Control Conference, Boston, Mass., Aug. 20-22, 1975; submitted March 11, 1975; revision received July 22, 1976.

Index categories: Aircraft Gust Loading and Wind Shear; Aircraft Landing Dynamics.

*Assistant Professor. Member AIAA.

†Professor and Chairman. Fellow AIAA.

Statistical Description of the Wind

The wind velocity (i.e. the velocity of the air with respect to the ground) cannot be predicted exactly at any given point in the atmosphere, so that a statistical description is appropriate. The wind velocity is considered to be a random vector at each point in space and time. A complete statistical description would not be tractable without simplifying assumptions and fortunately, several simplifications are reasonable:

1) The wind field is assumed to be stationary, horizontally homogeneous, and locally isotropic. 2) The variation in the wind with time and vertical position is considered negligible compared to the variation with horizontal position for an aircraft following a nearly horizontal path. 3) The correlations between wind velocity components at different horizontal positions are described by the von Karman model.[5] The wind structure is assumed to be dynamically similar throughout the atmospheric boundary layer. These simplifications are discussed in detail in Refs. 6-8 and, only the resulting statistical model for the mean and covariance of the wind will be presented here.

Application of the previous assumptions results in a model which depends upon four basic parameters: the surface roughness z_0, the velocity component variance σ^2, the turbulence scale L, and the direction of the mean wind ψ_w. Table 1 gives the surface roughness length for various types of terrain.

Table 1 Surface roughness for various types of surfaces[9]

Type of surface	$z_0(m)$
Mud flats, ice	$10^{-5} - 3 \cdot 10^{-5}$
Smooth sea	$2 \cdot 10^{-4} - 3 \cdot 10^{-4}$
Sand	$10^{-4} - 10^{-3}$
Snow	$10^{-3} - 6 \cdot 10^{-3}$
Mown grass	$10^{-3} - 10^{-2}$
Low grass, steppe	$10^{-2} - 4 \cdot 10^{-2}$
Fallow field	$2 \cdot 10^{-2} - 3 \cdot 10^{-2}$
High grass	$4 \cdot 10^{-2} - 10^{-1}$
Palmetto	$10^{-1} - 3 \cdot 10^{-1}$
Suburbia	1 – 2
City	1 – 4

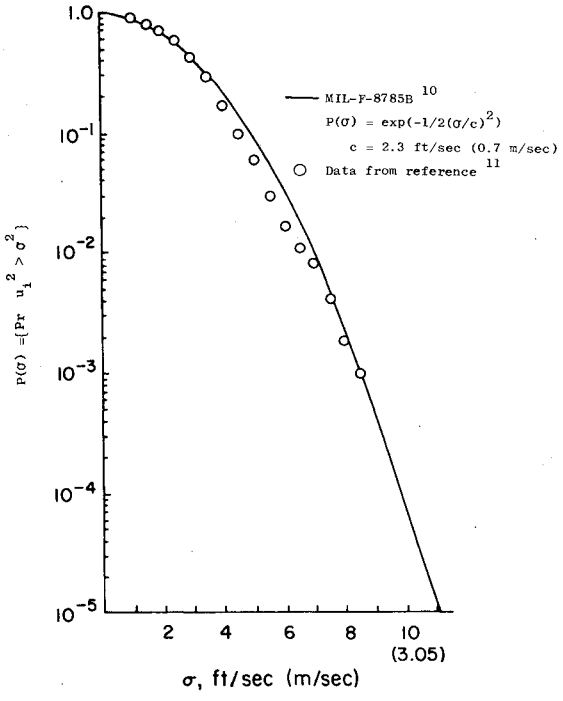

Fig. 1 Probability distribution of the rms turbulent velocity.

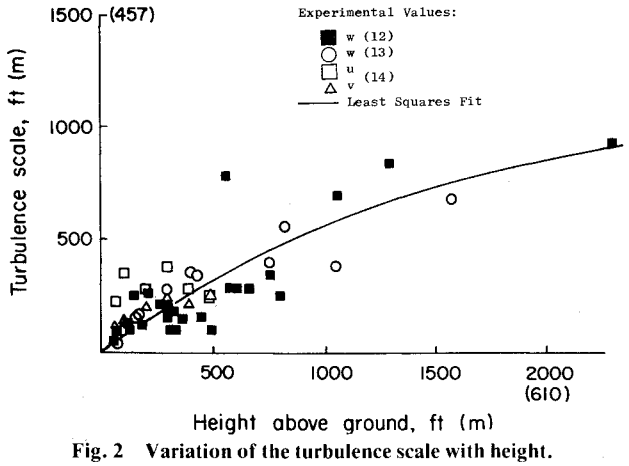

Fig. 2 Variation of the turbulence scale with height.

Figure 1 shows a probability distribution for the velocity component variance suggested in the military specification MIL-F-8785B [10] and data reported by Gault and Gunter. [11]

Figure 2 shows the variation in the turbulence scale with height for data from several sources. [12-14] Here, the scale L is defined by

$$L=\int_0^\infty f(r)\,dr$$

where $f(r)$ is the longitudinal correlation function normalized by the variance. A least-squares fit to the data results in the following equation

$$L=0.8\frac{(760\text{m})z}{(760\text{m})+z}$$

Due to scatter in the data, this equation should be recognized as describing only the character of the variation of scale with height not as a hard and fast physical law.

The direction of the mean wind will depend upon local conditions and the flight path chosen as the reference axis. For approach and landing, it is desirable that the mean wind be directed along the runway. However, landing difficulty is increased as the wind direction becomes normal to the runway, so this direction will be adopted.

Once the four parameters above are specified, the complete mean and correlation model of the wind, based on the previous assumptions, becomes

$$U_x = \cos\psi_w \frac{\sigma}{0.8}\ln\frac{z}{z_0}$$

$$U_y = \sin\psi_w \frac{\sigma}{0.8}\ln\frac{z}{z_0}$$

$$R_{uu}(\xi,\eta,z) = \sigma^2\left[f(r)+\frac{1}{2}\frac{\eta^2}{r}\frac{d}{dr}f(r)\right]$$

$$R_{vv}(\xi,\eta,z) = \sigma^2\left[f(r)+\frac{1}{2}\frac{\xi^2}{r}\frac{d}{dr}f(r)\right]$$

$$R_{ww}(\xi,\eta,z) = \sigma^2\left[f(r)+\frac{1}{2}r\frac{d}{dr}f(r)\right]$$

$$R_{uv}(\xi,\eta,z) = -\sigma^2\frac{1}{2}\frac{\xi\eta}{r}\frac{d}{dr}f(r)$$

$$R_{uw} = R_{vw} = 0$$

where U_x and U_y are the components of the mean wind velocity along the longitudinal (x) and lateral (y) flight path axes; R_{uu}, R_{uv}, etc. are the two-point turbulent velocity correlations for longitudinal and lateral separations, ξ and η, and height z; the subscripts u, v, w refer to the longitudinal, lateral, and vertical turbulent velocity components; and

$$r^2=\xi^2+\eta^2$$

$$f(r)=\frac{(2)^{2/3}}{\Gamma(1/3)}\mu^{1/3}K_{1/3}(\mu)$$

where

$$\mu = r/1.339L$$

$K_{1/3}(\mu)$ = modified Bessel function of order 1/3

A FORTRAN computer program was written to compute the mean velocity components and the turbulent velocity correlations according to the previous model and is given in detail in Ref. 6.

Aircraft Response to Atmospheric Turbulence

Even with a statistical model of the wind gusts, there still remains the nontrivial task of computing the statistical response of an aircraft flying through such a gust field. In virtually all analyses of aircraft gust response the incremental aerodynamic forces at each point on the aircraft are assumed to depend linearly upon the gust velocity field. In the pioneering work of Eggleston and Diederich [15] the concept was applied to an aircraft wing using lifting-line theory in the spatial domain. In most subsequent work, lifting surface theory is applied using the Fourier transform domain of spatial frequency. [16-19] The nonhomogeneity in the vertical direction makes the application of this technique difficult for descending flight paths. Also much of this work, particularly the more recent contributions, has emphasized structural responses for flight through the gust field. These responses are often characterized by complicated mode shapes, and large amounts of aerodynamic data are required in the analysis. Fortunately, in guidance and control applications considerable simplification is possible.

For many applications, a linear dynamical model of the aircraft based on the rigid body approximation is appropriate. Etkin[20] utilized the linearized rigid-body aircraft model and introduced the novel concept of approximating the turbulent gust field locally by a truncated Taylor series. Thus, in the spatial domain spanned by the aircraft, the gust velocity is approximated by the sum of uniform and gradient components. The forces and moments acting on the aircraft are given by linear influence coefficients closely resembling the usual aircraft "stability derivatives." Chalk et al.[10] present a set of rational approximations to the power-spectral densities for the uniform and gradient components given by Etkin. These approximations, based on the Dryden model for the turbulence,[21] are quite adequate for the uniform components, but they tend to underestimate the intensity of the gradient components.

A second approach, similar to that developed by Sketon,[22] is used here. The effective uniform and gradient components are found by averaging over several key points on the aircraft. It is found that as few as five points give a reasonable degree of approximation. This technique gives a straightforward method for determining the correlations for the uniform and gradient components based on the correlation model for the turbulent gusts. Once these correlations are determined, low-order linear shaping filters are found to approximate the correlations of the uniform and gradient components. The coefficients in these shaping filters depend upon one additional parameter, β, the ratio of aircraft size to turbulence scale. Because the analysis of linear systems forced by white noise is relatively straightforward, these models for the gust disturbances on the aircraft provide an effective tool for control system design.

Correlations for the Uniform and Gradient Components

The effective uniform and gradient components are found by averaging over the five points indicated in Fig.3.

The averaged components are given by

$$u_o = 1/5[u(\xi,\eta)+u(\xi+\xi_*,\eta)+u(\xi-\xi_*,\eta)$$
$$+u(\xi,\eta+\eta_*)+u(\xi,\eta-\eta_*)]$$

$$u_x = \frac{1}{2\xi_*}[u(\xi+\xi_*,\eta)-u(\xi-\xi_*,\eta)]$$

$$u_y = \frac{1}{2\eta_*}[u(\xi,\eta+\eta_*)-u(\xi,\eta-\eta_*)]$$

where u referes to the longitudinal gust velocity in aircraft path axes, and the subscripts 0, x, y refer to the uniform component and the longitudinal and lateral gradients, respectively.

Similar expressions are obtained for v_0, v_x, v_y, w_0, w_x, w_y, the lateral and vertical gust velocities and gradients. These equations represent estimates of the effective uniform and gradient components which minimize the sum of the squared velocity errors at the five points. Using these equations, the correlations of the uniform and gradient components are determined. For example

$$E\{u_y(\xi)u_y(\xi')\} = \frac{1}{2\eta_*}[R_{uu}(\xi-\xi',0)-R_{uu}(\xi-\xi',2\eta_*)]$$

The equations for all possible correlations are straightforward to calculate and are given in detail in Ref. 6. It now remains to determine appropriate positions in relation to the aircraft for the five points.

A reasonable approximation for the aerodynamic force distribution on an airplane is an elliptic lift distribution on the wind quarter-chord line plus two lifting points at the tail and nose. In Fig. 3 the points D and E are chosen to be at the tail and nose. Point A is chosen at the mass center. The points B and C are chosen so that the auto-correlation of the rolling moment (the quantity most affected by the placement of B and C), calculated using the three points on the wing, closely approximates the autocorrelation calculated using the elliptic lift distribution (as in Eggleston and Diedrich[15]). This gives a value of $\xi_* = 0.85b/2$. Figures 4 and 5 show the comparison for two values of the ratio of aircraft size to turbulence scale. The parameter β is defined as $b/2L$ or the wing semispan to turbulence scale ratio. Also shown in these figures are the correlations recommended by Chalk et al. in MIL-F-8785-B.[10] As can be seen in the figures, the correlations derived here, using the three-point approximation for the wing aerodynamics, are better approximations.

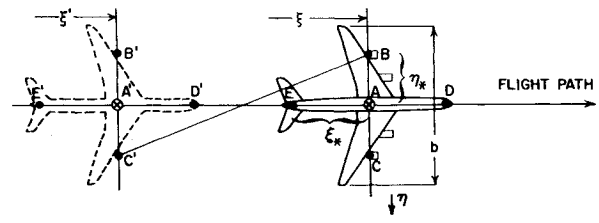

Fig. 3 Geometry of the five-point approximation.

Now, having determined an appropriate set of points for the approximation, all of the correlations between the various uniform and gradient components can be determined. However, the correlations so derived are still in a form which is difficult to apply in practice. In order to make the model more practical to use, linear shaping filters with output correlations approximating those just derived are determined. A general technique for finding an approximate linear shaping filter based on correlation data is presented in the Appendix. The following equations summarize the resulting model for the uniform and gradient gust disturbances which excite the lateral aircraft dynamics. Similar equations were derived for the longitudinal disturbances and are given in Ref. 6.

$$\frac{d}{d\xi}\begin{bmatrix} v_0 \\ v_x \\ u_y \\ w_y \end{bmatrix} = \begin{bmatrix} 0 & 1 & 0 & 0 \\ f_{21} & f_{22} & 0 & 0 \\ f_{31} & 0 & f_{33} & 0 \\ 0 & 0 & 0 & f_{44} \end{bmatrix}\begin{bmatrix} v_0 \\ v_x \\ u_y \\ w_y \end{bmatrix} + \begin{bmatrix} 0 & 0 & 0 \\ \gamma_{22} & \gamma_{23} & 0 \\ 0 & \gamma_{33} & 0 \\ 0 & 0 & \gamma_{44} \end{bmatrix}\begin{bmatrix} \eta_1 \\ \eta_2 \\ \eta_2 \\ \eta_3 \end{bmatrix}$$

where ξ is the distance along the path and η_i is white noise with correlation

$$E\{\eta_i(\xi_1)\eta_i(\xi_2)\} = \sigma^2 L\delta(\xi_1-\xi_2)$$

$$f_{21}L^2 = -(1+\beta)^{2/3}\beta^{-4/3}$$

$$f_{22}L = -0.5(1+3\beta)\beta^{-4/3}$$

$$f_{31} = -0.167 f_{21}$$

$$f_{33}L = -0.4(1+2\beta)/\beta$$

$$f_{44} = 1.5 f_{33}$$

$$\gamma_{22} = -f_{21}$$

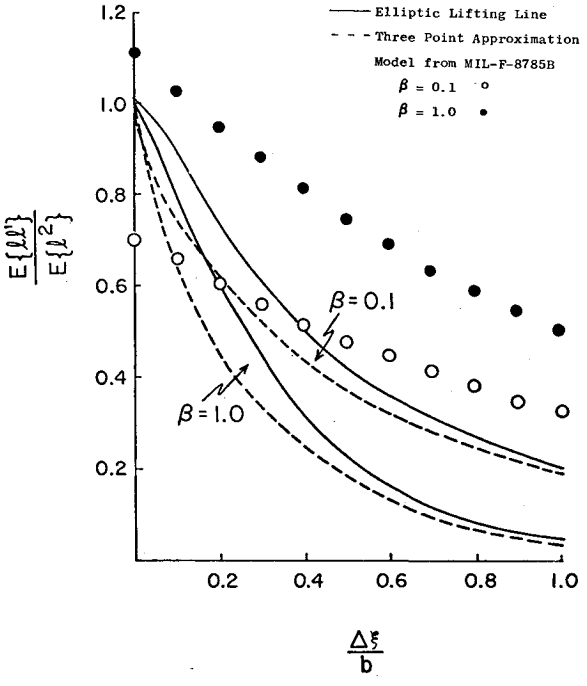

Fig. 4 Normalized correlations for the wing rolling moment.

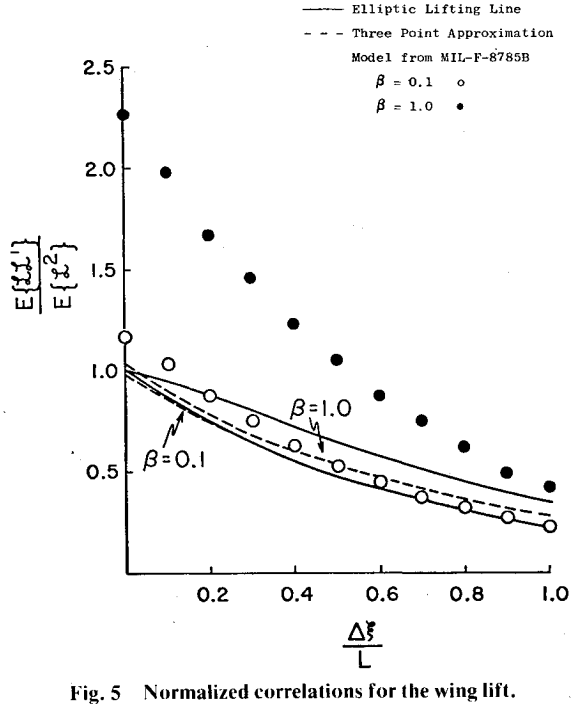

Fig. 5 Normalized correlations for the wing lift.

$$\gamma_{23}L^2 = -0.23\beta^{-4/3}$$

$$\gamma_{33}L^2 = 1.33/\beta$$

$$\gamma_{44}L^2 = 1.67/\beta$$

These functions of β were determined by rounding the parameters determined by a least-squares fit using a function of the form

$$f(\beta) = a_1(1+a_2\beta)^{a_3}\beta^{a_4}$$

Figures 6 a through 6c show a comparison of some of the correlations for the linear shaping filters and for the five-point averaged correlation model. The sharp peaks in the correlations for the five-point approximation occur because of the discrete approximation. The correlations for the linear shaping filters are seen to be smooth approximations to the five-point correlations.

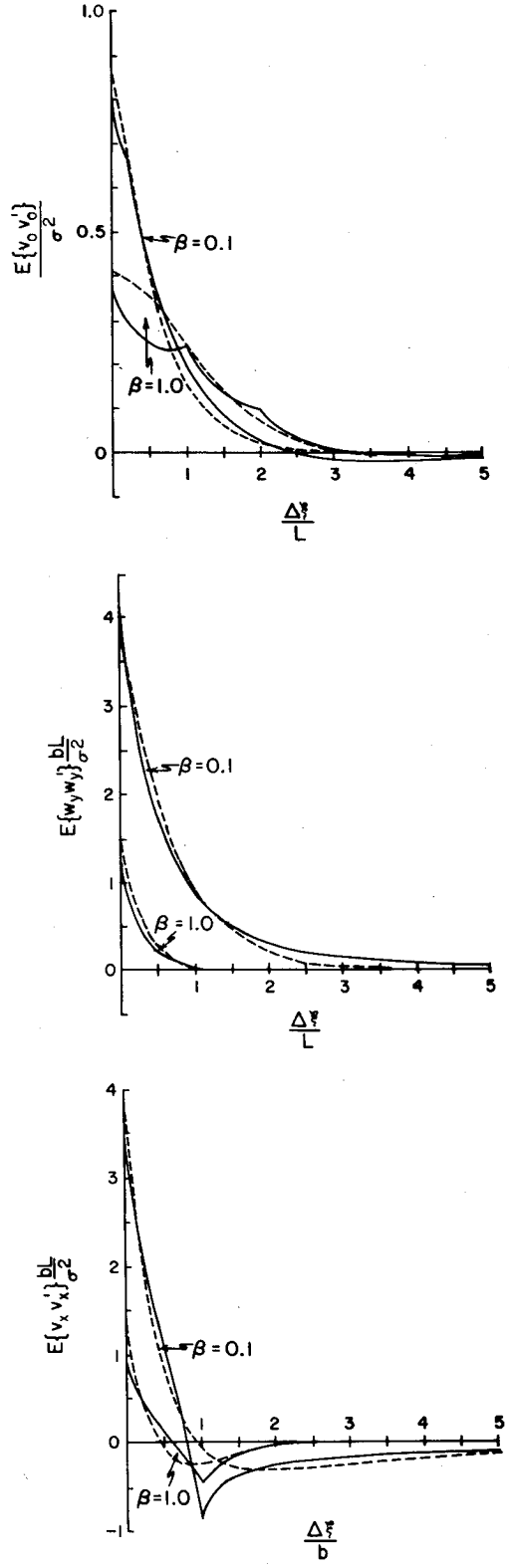

Fig. 6 Correlations for the lateral gust inputs.

Lateral Autopilot Design for Landing in a Crosswind

The lateral motions of a DC-8 aircraft during an automatic decrab maneuver are now investigated. Quadratic optimal

control design techniques were used' assuming accurate information regarding the lateral aircraft state variables (position, velocity, attitude, and attitude rates) to be available. Obviously this is the limiting case that gives the best possible performance.

Steady Crabbed and Decrabbed Flight

The decrab maneuver takes the aircraft from steady crabbed flight (zero sideslip with respect to the air and zero roll angle) to steady decrabbed flight (zero sideslip with respect to the ground and nonzero roll angle), while maintaining the horizontal component of the aircraft velocity parallel with the runway centerline. The required initial crab angle and final roll angle and control deflections are readily calculated from static force and moment considerations. Thus, the initial crab angle is given by

$$\psi_c = -U_y/V$$

where U_y = mean lateral wind velocity and V = aircraft velocity. For the DC-8 aircraft the final roll angle and control deflections are given by

$$\varphi = -.459\,U_y/V$$

$$\delta a = -1.30\,U_y/V$$

$$\delta r = 2.12\,U_y/V$$

Quadratic Optimal Design

For the quadratic optimal design procedure, a performance index is chosen which appropriately weights the aircraft attitude and path deviations against the control. The performance index is then optimized, subject to the constraints of the aircraft dynamics. For the case of the decrab autopilot, a reasonable choice for the performance index is

$$J = \frac{1}{2}\int_0^\infty \left[\left(\frac{y}{y_*}\right)^2 + \left(\frac{\psi}{\psi_*}\right)^2 + \left(\frac{\delta a}{\delta a_*}\right)^2 + \frac{\delta r}{\delta r^*}\right]$$

Choosing the weighting factors

$$y_* = 15 \text{ ft } (4.6\text{m})$$

$$\psi_* = 2 \text{ deg } (.035\text{rad})$$

$$\delta a_* = 10 \text{ deg } (.17\text{rad})$$

and

$$\delta r^* = 10 \text{ deg } (.17\text{rad})$$

yields the control law

$$\delta a = -3.57\varphi' - 2.47\varphi - 4.63\psi' - 1.60\psi - 8.55\epsilon - 0.659y$$

$$\delta r = -0.233\varphi' - 0.496\varphi - 9.19\psi' - 3.63\psi - 2.92\epsilon - 0.0996y$$

where φ, ψ, and ϵ are the roll, yaw, and path azimuth angles (deg), φ' and ψ' are the roll and yaw rates (deg/hft), δa and δr are the aileron and rudder deflections (deg), and y is the lateral position (ft). The independent variable is distance along the path, ξ, measured in units of hundred-feet (hft). The closed-loop poles using this control law are shown in Fig. 7.

In the presence of a steady crosswind, this control law will give undesirable steady offsets. To remove the steady offset, the control law is augmented with integrals of the lateral position and yaw attitude deviations. In order to keep the closed-loop characteristics as prescribed by the quadratic optimization procedure, a linear combination of the aircraft states is added to each control. The resulting control law, with

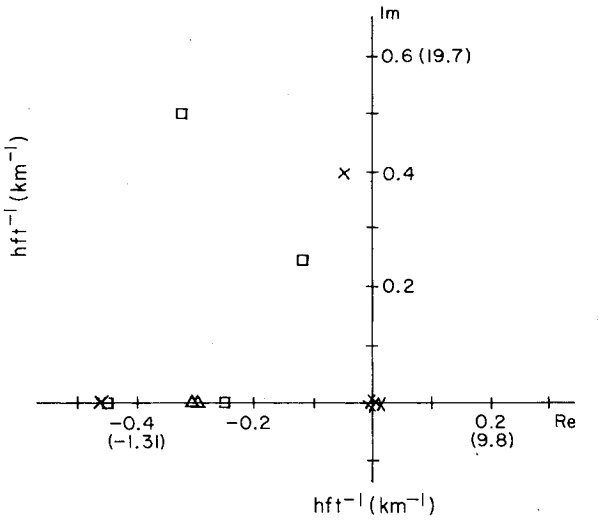

Fig. 7 Closed-loop poles for the quadratic optimal law, where × = open-loop poles, □ = closed-loop poles, and Δ = additional poles for integral control action.

the additional closed-loop poles due to the integral action chosen as shown in Fig. 7, is

$$\delta a = -5.796\varphi' - 4.567\varphi - 7.703\psi' - 2.768\psi$$
$$- 22.21\epsilon - 2.547y - 0.1978\bar{y} + 0.2502\bar{\psi}$$

$$\delta r = 0.1203\varphi' - 0.6733\varphi - 14.01\psi' - 6.995\psi$$
$$- 5.658\epsilon - 0.2750y - 0.0298\bar{y} - 1.657\bar{\psi}$$

$$d\bar{y}/d\xi = y$$

$$d\bar{\psi}/d\xi = \psi$$

A more detailed discussion of this control law is given in Ref. 23. An interesting property of the control law is that it is equivalent to estimating the offset due to the constant disturbance with a reduced-order observer and feeding this estimate back using the quadratic-optimal control law.

Mean Response for the Decrab Maneuver

Using the logarithmic wind profile discussed earlier, the mean response of the aircraft under autopilot control can be computed. A value of 3.5 ft/sec (1.1 m/sec.) is chosen for the friction velocity. This value corresponds to a value of rms turbulent gust velocity of 7 ft/sec, which is exceeded only one percent of the time (see Fig. 1), and yields a wind shear of 14 ft/sec/hft which is at the top of the moderate range as classified by the ICAO.[24] A value of 5 ft (1.5m) for the roughness length is chosen as typical of a suburban environment (see Table 1). Assuming the wheel height profile shown in Fig. 8, the crosswind is determined as a function of range. This height profile assumes a flare which begins at a height of 50 ft (15m) and which linearly reduces the glide slope from 3 deg (0.05 rad) tp 0.5 deg (0.008 rad) just before touchdown.

The mean response for the decrab maneuver using the integral-augmented optimal design for the DC-8 aircraft is shown in Fig. 9. The initial conditions are chosen to be the nominal configuration at the end of the approach. The lateral position and path angle are aligned with the runway centerline, the wings are level, and the yaw attitude is crabbed into the wind. The initial conditions on the integrators of lateral position and yaw attitude are chosen to provide a continuous

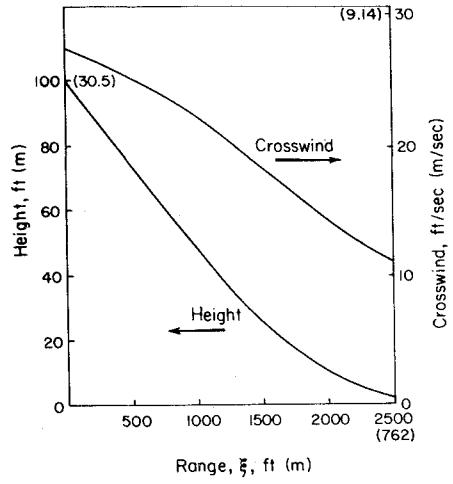

Fig. 8 Crosswind variation with range.

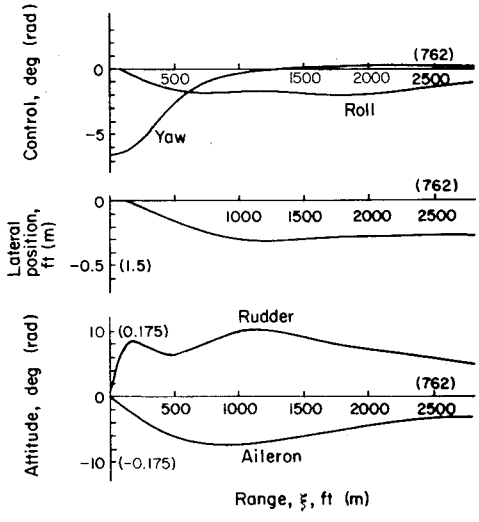

Fig. 9 Mean lateral response for the integral-augmented optimal design.

control at the initiation of the decrab maneuver. The maneuver is performed smoothly with only slight offsets in yaw and position. These small offsets result because the height-dependent crosswind acts as a ramp input to the "type-1" controller. The small roll angle is necessary to maintain the required aerodynamic sideslip without allowing the aircraft to drift sideways with respect to the ground.

Turbulent Gusts (rms Lateral Aircraft Response)

In order to determine whether advantage can be taken of the ability to predict ahead using the statistical model of the turbulence, the behavior of the aircraft is analyzed using minimum-variance control theory. If the models for the effective gust disturbances are combined with the linearized lateral aircraft equations, a tenth-order linear system forced by white noise results. An important result of optimal control theory states that the optimal control law for a performance index equal to the expected value of an integrated quadratic form in the state and control is a linear function of the state and does not depend upon the white noise disturbances.[25,26] Using the expected value of the performance index used in the previous quadratic-optimal control design, the optimal control law including feedback of the wind states can be determined. Several important properties of this control law and the resulting aircraft response should be noted. First, the feedback gains for the aircraft states do not depend upon the gust disturbance model. Second, the feedback gains for the wind

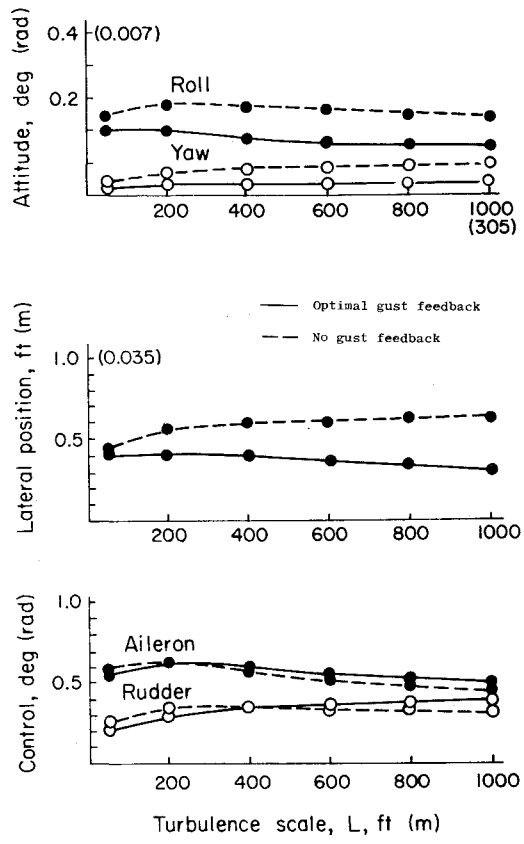

Fig. 10 One ft/sec rms turbulence (rms lateral aircraft response).

states do not depend upon the rms turbulent velocity. Third, the covariance of the controlled aircraft response depends linearly on the variance of the turbulent gust velocity.

The controlled rms aircraft response for an rms gust velocity of 1 ft/sec (0.3m/sec) using the optimal gust feedback for various values of the turbulence scale is shown in Fig. 10. For comparison purposes, the rms aircraft response using only the feedback of aircraft states (the optimal control for purely random, white-noise wind gusts), is also shown in the figure. For larger values of turbulence scale, significant improvement in the rms aircraft response can be made by feeding back the wind states. However, near the ground when the turbulence scale is relatively small, little improvment is made.

The previous results assumed the gust inputs to be a stationary process. During the approach and decrab maneuver, the turbulence scale gets smaller and smaller as the height is reduced. Since this reduction in height is considerably smaller than the horizontal distance traveled, the use of the linear shaping filter model is still appropriate, except that the turbulence scale parameter is made to vary with height. Using the same height profile as in the mean response calculation, the rms aircraft response as a function of range is shown in Fig. 11. The integral-augmented optimal control law is used and the initial covariances are taken to be the stationary optimal values from the previous results. The rms turbulent velocity is taken to be the 99% confidence value of 7 fps (2.1 m/sec). The resulting rms lateral position of 1.2 ft (0.37m) at touchdown is an order of magnitude below the value of 13 ft (4m) suggested for autoland systems by the FAA. It must be remembered, however, that the FAA value includes the lateral dispersion due to all sources of error. The excellent performance of the integral-augmented, optimal controller for wind disturbances indicates that it should be possible with accurate navigation sensors to be well within the accuracy required for Category III (zero visibility) automatic landings.

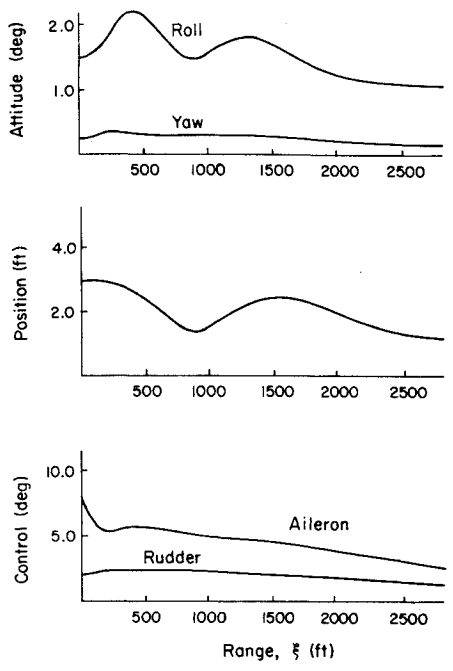

Fig. 11 Altitude-dependent turbulence (rms lateral response).

Summary and Conclusions

In the first section, the available information on the statistical characteristics of the wind was reviewed. It was found that the logarithmic mean wind profile and the isotropic von Karman correlation functions for the turbulent fluctuations describe the wind reasonably well. Very near the ground, there are some deviations from the isotropic behavior, but in the absence of a better three-dimensional model, the isotropic relations were used throughout. Future work could be well spent in determining an improved engineering model of the three-dimensional wind gust correlations in the surface layer.

In the second section, a systematic procedure was developed for approximating the forces and moments due to the atmospheric turbulence acting on the aircraft. The resulting linear shaping filters provide a model for both the analysis of the aircraft's response to the mean wind shear and turbulence and the effective design of practical autopilots. This model, for the first time, incorparates the full three-dimensional character of the turbulence based on the von Karman model in a form which is also practical to use for auto-pilot design.

The third section dealt with the design of lateral autopilots for landing an aircraft in the presence of a crosswind. The effects of both the mean wind shear and the resulting turbulence were considered. It was found that the optimal control design technique provides an effective method for choosing the basic structure as well as optimizing the parameters for such a complicated multiloop system. To provide improved response in the presence of the mean wind, integral-error states were added. The nonstationary rms response was determined for a DC-8 aircraft which showed an rms lateral touchdown dispersion of only 1.2 ft. (0.37m) due to wind gust effects.

Appendix: Determination of a Linear Shaping Filter to Match Given Correlation Data

Suppose a vector process x satisfies a set of linear differential equations

$$dx/d\xi = Fx + \Gamma\eta$$

where η is white noise with zero mean and correlation

$$E\{\eta(\xi_1)\eta^T(\xi_2)\} = qI\delta(\xi_1 - \xi_2)$$

The state covariance, $\chi(\xi) = E\{xx^T\}$, is then given by

$$d\chi/d\xi = F\chi + \chi F^T + q\Gamma\Gamma^T$$

and the correlation function

$$C(\xi_1,\xi_2) = E\{x(\xi_1)x^T(\xi_2)\}$$

by

$$\frac{d}{d\xi}C(\xi,\xi_1) = FC(\xi,\xi_1)$$

$$C(\xi_1,\xi_1) = \chi(\xi_1)$$

Integrating the correlation equation for constant F yields

$$C(\xi_2,\xi_1) - \chi(\xi_1) = F\int_{\xi_1}^{\xi_2} C(\xi,\xi_1)\,d\xi$$

or

$$F = [C(\xi_2,\xi_1) - \chi(\xi_1)]\left[\int_{\xi_1}^{\xi_2} C(\xi,\xi_1)\,d\xi\right]^{-1}$$

This equation can now be used to compute the system dynamics matrix F, given the state correlation $C(\xi,\xi_1)$. In cases when F may be slowly varying, the equation can also be used providing the interval (ξ_1,ξ_2) is chosen small enough. Once an appropriate F matrix is determined, the disturbance distribution matrix Γ can be determined from the covariance equation

$$\Gamma\Gamma^T \approx -\frac{1}{q}(F\chi + \chi F^T)$$

To provide a unique result, Γ is chosen to be upper triangular and q is chosen to be any convenient value.

Acknowledgment

This research was supported by NASA under Grant NGL 05-020-007.

References

[1] Bleeg, R.J., Tisdale, H.F., and Virks, R.M., "Inertially Augmented Automatic Landing System," FAA Report No. FAA-RD-72-22, 1972.

[2] Mackinnon, D. and Madden, P., "Performance Limits of a Radio-Intertial Lateral Control System for Automatic Landing," *Journal of Aircraft*, Vol 9., Aug. 1972, pp. 513-520.

[3] Anon., "Microwave Scanning Landing Guidance System (LGS)," R.T.C.A. Special Committee 117 paper 189-70, 1970.

[4] Kayton, M. and Fried, W., *Avionics Navigation Systems,* Wiley, New York, 1969, pp. 421-443.

[5] von Karman, T., "Sur la Theorie Statistique de la Turbulence," *Computes Rendus des Seances de l'Academie des Sciences,* Vol. 226, 1948, pp. 2108-2111.

[6] Holley, W.E. and Bryson, A.E., "Wing Modeling and Lateral Aircraft Control for Automatic Landing,", Stanford University, Stanford, Calif., Dept. of Aeronautics and Astronautics, SUDAAR No. 489, Jan. 1975.

[7] Tennissen, H.W., "Characteristics of the Mean Wind and Turbulance," Univ. of Toronto, UTIAS Review No. 32, Oct. 1970.

[8] Lumley, J.L. and Panofsky, H.A., *The Structure of Atmospheric Turbulence,* Wiley, New York, 1964.

[9] Fichtl, G.H., "Wind Shear Near the Ground and Aircraft Operations," *Journal of Aircraft*, Vol. 9, Nov. 1972, p. 766.

[10] Chalk, C.R., Neal, T.P., Harris, T.M., Pritchard, F.E., and Woodcock, R.J., "Background Information and User Guide for MIL-F-8785B(ASG)," AFFDL-TR-69-72, Aug. 1969, pp. 440-442.

[11] Gault, J.D. and Gunter, D.E., "Atmospheric Turbulence Considerations for Future Aircraft Designed to Operate at Low Altitudes," *Journal of Aircraft,* Vol. 5, Dec. 1968, p. 577.

[12]Taylor, R.J., Warner J., and Bacon, N.C. "Scale Length in Atmospheric Turbulence as Measured From an Aircraft, "*Quartely Journal of the Royal Meteorological Society*, Vol. 96, 1970, pp. 750-755.

[13]Busch, N.E. and Panofsky, H.A., "Recent Spectra of Atmospheric Turbulence," *Quarterly Journal of the Royal Meteorological Society*, Vol. 94, 1968, pp. 132-148.

[14]Fichtl, G.H. and McVehil, G.E., "Longitudinal and Lateral Spectra of Turbulence in the Atmospheric Boundary Layer," NASA-TN-D-5584, Feb. 1970.

[15]Eggleston, J.M. and Diederich, F.W."Theoretical Calculations of the Power Spectra of the Rolling and Yawing Moments on a Wing in Random Turbulence," NACA Report 1321, 1957.

[16]Ribner, H.S., "Spectral Theory of Buffeting and Gust Response: Unification and Extension," *Journal of Aeronautical Science,* Vol. 23, Dec. 1956, pp. 1075-1077.

[17]Houbolt, J.C., Steiner, R., and Pratt, K.G., Dynamic Response of Airplanes to Atmospheric Turbulence Including Flight Data on Input and Response, NASA TR-R-199, 1964.

[18]Filotas, L.T., "Approximate Transfer Functions for Large Aspect Ratio Wings in Turbulent Flow," *Journal of Aircraft*, Vol. 8, June 1971, pp. 395-400.

[19]Eichenbaum, F.D., "A General Theory of Aircraft Response to Three-Dimensional Turbulence," *Journal of Aircraft*, Vol. 8., May 1971, pp. 353-360.

[20]Etkin, B., "Theory of Flight of Airplanes in Isotropic Turbulence-Review and Extension," AGARD Report 372, 1961.

[21]Dryden, H.L., "Turbulence Investigations at the National Bureau of Standards," *Proceedings of the 5th International Congress of Applied Mechanics,* 1938, p. 365.

[22]Skelton, G.B., "Investigation of the Effects of Gusts on VSTOL Craft in Transition and Hover," AFFDL-TR-68-85, 1968, pp. 57-61.

[23]Holley, W.E. and Bryson, A.E., "Multi-Input, Multi-Output Regulator Design for Constant Disturbances and Non-Zero Set Points with Application to Automatic Landing in a Crosswing," Dept. of Aeronautics and Astronautics, Stanford University, Stanford, Calif., SUDAAR No. 465, Aug. 1973, pp. 17-23.

[24]Anon.,

[25]Bryson, A.E. and Ho, Y.C., *Applied Optimal Control*, Blaisdell, New York, 1969, pp. 408-412.

[26]Kwakernaak, H. and Sivan, R., *Linear Optimal Control Systems*, Wiley, New York, 1972, pp. 259-263.

[27]Anon., "Automatic Landing Systems" FAA Advisory Circular 20-57A, 1971.